Carbohydrate Polymers 112 (2014) 448–457

Contents lists available at ScienceDirect

Carbohydrate Polymers

journal homepage: www.elsevier.com/locate/carbpol

Chemo-selective high yield microwave assisted reaction turns cellulose to green chemicals

Salman Hassanzadeh, Nina Aminlashgari, Minna Hakkarainen*

Department of Fibre and Polymer Technology, School of Chemical Science and Engineering, KTH Royal Institute of Technology, SE-100 44 Stockholm, Sweden

ARTICLE INFO

Article history:
Received 19 April 2014
Received in revised form 6 June 2014
Accepted 7 June 2014
Available online 14 June 2014

Keywords:
Cellulose
Liquefaction
Glucose
Levulinic acid
Hydrothermal degradation
Carbon sphere

ABSTRACT

Exceptionally high cellulose liquefaction yields, up to 87% as calculated from the amount of solid residue, were obtained under mild conditions by utilizing the synergistic effect of microwave radiation and acid catalysis. The effect of processing conditions on degradation products was fingerprinted by rapid laser desorption ionization-mass spectrometry (LDI-MS) method. The reaction was chemo-tunable, enabling production of glucose (Glc) or levulinic acid (LeA) at significantly high selectivity and yields, the relative molar yields being up to 50 and 69%, respectively. A turning point from pure depolymerization to glucose to further degradation to levulinic acid and formic acid was observed at approximately 50% liquefaction or above 140 °C. This was accompanied by the formation of small amounts of solid spherical carbonized residues. The reaction was monitored by multiple analytical techniques. The high yields were connected to the ability of the process to break the strong secondary interactions in cellulose. The developed method has great potential for future production of green platform chemicals.

1. Introduction

Sustainable production of fuels, chemicals and materials is one of the most strategically important research fields at the moment. Future supply of materials and energy need to be ensured at the same time as carbon dioxide emissions should be reduced. Lignocellulosic biomasses are among the most promising renewable resources for production of biofuels and bio-based platform chemicals, as they are widely available and do not compete with the food supply (Chheda, Huber, & Dumesic, 2007). Studies on hydrolysis of cellulose to its sugar building blocks and other valuable chemicals were performed already in the late 19th century (Monier-Williams, 1921; Ritter, Mitchell, & Seborg, 1933; Simonsen, 1898). However, a truly cost-effective and controllable process for liquefaction or depolymerization of cellulose to desired chemicals is still lacking, and could revolutionize the commercialization and large-scale production of bio-based platform chemicals (Chundawat et al., 2011; Himmel et al., 2007; Matson, Barta, Iretskii, & Ford, 2011).

Different strategies have been evaluated to achieve effective liquefaction of cellulose (Sun & Cheng, 2002). These include treatment with reconstructive chemicals e.g. high concentrated acidic (Ritter et al., 1933; Xiang, Lee, Pettersson, & Torget, 2003) or basic (Knill & Kennedy, 2003) solutions, in alcohols (Lin, Yao, Yoshioka, Shiraishi, & 2004), highly ionic medium (Pinkert, Marsh, Pang, & Staiger, 2009), steam explosion (Carrasco, Sáiz, Navarro, Soriano, Sáez, & Martinez, 1994), harsh physical hydrolysis conditions e.g. supercritical water (Sasaki, Fang, Fukushima, Adschiri, & Arai, 2000), high temperatures (Bobleter, Niesner, & Röhr, 1976), different catalysis systems e.g. homogenous and/or heterogeneous acids (Huang & Fu, 2013) and enzymes (Hendriks & Zeeman, 2009). An advantage with enzyme-catalyzed hydrolysis is the high selectivity. However, it suffers from low efficiency and high cost. Concerning chemical catalysis, acid hydrolysis is usually preferred in comparison to alkaline hydrolysis, due to lower amount of side reactions and higher yields (Chheda et al., 2007).

The structure–property studies performed on the native cellulose strongly propose that the main barrier for hydrolysis and depolymerization of α-cellulose chains in the aqueous medium are the protected β(1-4)-glycosidic linkages within crystalline (I) structure and inter chain, intra chain and inter sheet networks of hydrogen bonding (Chundawat et al., 2011; Takahashi &

Abbreviations: Glc, glucose; LeA, levulinic acid; LeNa, sodium levulinate; FA, formic acid; HMF, hydroxymethylfurfural; PTSA, *p*-toluenesulfonic acid monohydrate; *A*, acid concentration; *C*, amount of cellulose; *T*, temperatures; *t*, holding time; LY, liquefaction yield; CI, crystallinity index; TAC, total weight of the amorphous cellulose; TAA, total amorphous area; DCA, decrystallized area; DCE, decrystallization efficiency; FTIR, Fourier transform infrared; NMR, nuclear magnetic resonance; XRD, X-ray diffraction; LDI-MS, laser desorption ionization-mass spectrometry.

* Corresponding author. Tel.: +46 87908271.
E-mail addresses: salmanha@kth.se (S. Hassanzadeh), ninaam@kth.se (N. Aminlashgari), minna@kth.se (M. Hakkarainen).

http://dx.doi.org/10.1016/j.carbpol.2014.06.011
0144-8617/

Matsunaga, 1991). The depolymerization process in the crystalline segments of α-cellulose follows two subsequent steps: the dissolution of the highly ordered chains and hydrolysis of the glycosidic positions (Hilgert, Meine, Rinaldi, & Schuth, 2013). The most efficient depolymerization of cellulose will be achieved if disruption of the hydrogen bonding and, thus, softening (dissolving) of the highly ordered cellulose chains occurs, and the required activation energy for hydrolytic cleavage of the β-1,4-glycosidic bonds between two anhydroglucose units is provided (Liu et al., 2013).

The methods to dissolve cellulose during the hydrolysis procedure include (1) highly ionic solvents (such as concentrated O-rich acids, bases or ionic liquids) and (2) high-temperature dissolution in sub- or supercritical water (Ogihara, Smith, Inomata, & Arai, 2005; Sasaki et al., 2000). Up-scaling these processes suffer from several disadvantages such as: not being green, costly, uncontrollable and non-selective processes which often contain several steps. Other problems can also be connected to reactor corrosion, difficult catalyst recovery and low yields.

Microwave assisted reactions have appeared as highly attractive means for chemical degradation of polymers and liquefaction of biomass (Allan, Krieger, & Work, 1980; Sequeiros, Serrano, Briones, & Labidi, 2013). Wood liquefaction in glycols with *p*-toluenesulfonic acid as catalyst has also been carried out (Azwar, Yin, & Hakkarainen, 2013; Kržan & Žagar, 2009). However, the disadvantage of this process is the large amount of glycols needed and it is, therefore, mainly suitable for applications such as thermoset production, where the whole liquefaction product inclusive the glycols can be utilized without further purification. In more recent work microwave-assisted conversion of carbohydrates to levulinic acid (LeA) was evaluated by acid catalyzed microwave-assisted reaction (Szabolcs, Molnar, Dibo, & Mika, 2013). Liquefaction of cellulose, chitin and chitosan was evaluated and 34.2% conversion of cellulose to levulinic acid was reported. Direct microwave-assisted hydrothermal depolymerization without any catalysts was also investigated at 150–270 °C (Fan et al., 2013; Moller, Harnisch, & Schroder, 2013). The authors found that only the amorphous cellulose was susceptible to depolymerization at temperatures below 220 °C, resulting in maximum liquefaction and glucose (Glc) yields of 14% and 11% at 220 °C, respectively. Increasing the temperature to 250 °C increased the glucose yield to 21% but decreased the selectivity of glucose production from 75% to 36%.

While the previous studies are promising, there is still space for large improvements with respect to the efficiency of the process to achieve more complete and more chemo-selective reactions under as mild conditions as possible. Here we introduce a strategy to reach dissolution–depolymerization of cellulose in water through synergistic function of dilute acid catalyst and microwave radiation at moderate temperatures aiming at effective high-yield chemoselective conversion of cellulose to valuable green chemicals. At the same time laser-desorption ionization-mass spectrometry (LDI-MS) was shown to be rapid and excellent tool for fingerprinting the liquefaction products.

2. Experimental

2.1. Materials

α-Cellulose (C) (product no. C8002) commercial grade containing 3% of pentose (Xylan) (Xiang et al., 2003) was obtained from Sigma–Aldrich and dried under vacuum overnight (25 °C) before use. Levulinic acid (LeA) (>97%), α-D-glucose (anhydrous, 96%), sulfuric acid (H_2SO_4) (95–98%), *p*-toluene sulfonic acid monohydrate (PTSA) (98%) and sodium hydroxide (NaOH) (>98%) were purchased from Sigma–Aldrich and were used as received. Deuterium oxide was obtained from Cambridge Isotope Laboratories (99.9%). Deionized water was used as a solvent for all the liquefaction reactions.

2.2. Microwave assisted liquefaction

The different catalysts (NaOH, H_2SO_4, LeA and PTSA) were first evaluated for their efficiency to liquefy cellulose. The reactions were performed during constant temperature at 140 °C for 2 h. Based on these results the optimization of the process with sulfuric acid as the main catalyst was then performed by systematically changing the following parameters; acid concentration (0.0025, 0.005, 0.01, 0.02 or 0.04 g/ml) (*A*), amount of cellulose (0.1, 0.5, 1.0 and 2.0 g) (*C*), temperatures (100, 120, 140, 160 and 180 °C) (*T*), and liquefaction time at set temperature, holding time (30, 60, 90, 120 and 160 min) (*t*). All the reactions were accomplished in a MES-1000 (CEM Corporation) microwave with a maximum power of 950 W ± 50. The materials were reacted in 100 ml Teflon PFA vessels, filled with 20 ml of liquefaction solvent. Temperature and pressure were measured in one of the vessels by optical probe. The experiments were performed in dynamic mode, where the microwave will reach and keep the desired temperature by input irradiation and with full power effect (100%) while the maximum pressure was set to 150 psi and RAMP-time to 20 min. After each reaction, the tubes were cooled down in an ice bath before they were opened. The samples were filtered and the precipitate was washed with 20 ml of distilled water to separate the liquefied products from the remaining residue. The liquefied products were neutralized with NaOH for further analysis. The solid residue was dried overnight and kept in vacuum oven for further gravimetrical analysis. The liquefaction yield (LY) was calculated from the weight of the solid residue (original cellulose residue and/or formed solid carbon spheres):

$$LY\ \ (\%) = \frac{(\text{Original cellulose}\ \ (\text{g}) - \text{Residue}\ \ (\text{g}))}{\text{Original cellulose}\ \ (\text{g})} \times 100$$

2.3. Characterization

Fourier transform infrared (FTIR) spectra of liquefied products and residues were recorded on a Perkin Elmer Spectrum 2000-spectrometer (Perkin Elmer Instrument) with 16 scans at a resolution of 4 cm^{-1}. Nuclear magnetic resonance, ^1H NMR (400.13 MHz; Me_4Si) and ^{13}C NMR (100.62 MHz; Me_4Si) spectra were recorded on a Bruker Avance 400 spectrometer at 298 K. For the analysis, approximately 20 mg (^1H NMR) or 120 mg (^{13}C NMR) of the vacuum dried liquefied product was dissolved in 1 ml of D_2O. In addition to determining the liquefaction yield from the amount of remaining solid residue, the total weight of all water-soluble organic degradation products was determined by evaporating the liquefaction solvent (water) and weighting the remaining residue. The total weight of the organic water-soluble liquefaction products was obtained after a weight reduction corresponding to the theoretical amount of formed Na_2SO_4 based on the added H_2SO_4 and NaOH. The total amount of organic degradation products was then correlated to the molar composition extracted from ^1H NMR to determine the relative molar yield of each product in relation to starting materials from:

$$\text{Relative Yield}\ \ (\text{mol}\%) = \frac{\text{Actual Molar Yield}}{\text{Theoretical Yield}} \times 100\%$$

UV–vis spectra of the liquefied products were recorded on a UV-2401 UV–Vis spectrophotometer with deionized water as reference samples. A Bruker UltraFlex time-of-flight mass spectrometer with a SCOUT-MTP ion source (Bruker Daltonics, Bremen, Germany) in reflector mode equipped with a 337 nm nitrogen laser was used for the laser desorption ionization-mass spectrometry (LDI-MS)

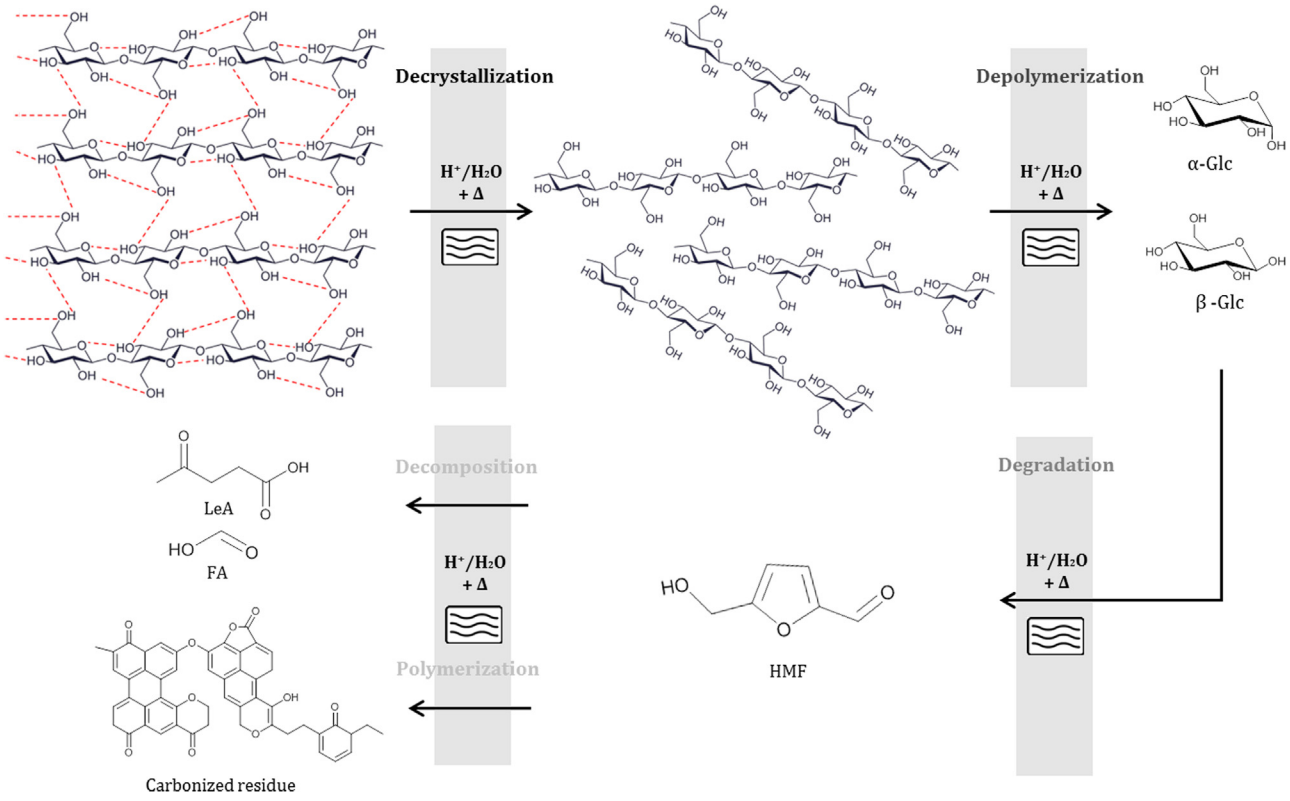

Fig. 1. Summary of the acid catalyzed-microwave-assisted cellulose liquefaction process.

analysis of the liquefied products. 0.5 μL of the neutralized sample medium was directly applied on the stainless steel plate and allowed to evaporate before analysis. The acceleration voltage was 25 kV and the reflector voltage 26.3 kV. All experiments were run in positive ion mode. The spectrum obtained for each sample is an accumulation of 1000 laser shots at different spots. The mass-to-charge (m/z) ratio range was set to scan from 60 m/z to 2000 m/z.

X-ray diffraction (XRD) spectra of the original cellulose sample and solid residues were recorded with CuKR radiation ($\lambda = 0.1541$ nm) using a PANalytical XPert Pro instrument at 25 °C with a silicium mono-crystal sample holder at the step size of 0.017°. The intensity (Miller indices) as a function of 2θ was measured while the angle range was 5–40°. The crystallinity index (CI) was measured by Segal method (Segal, Creely, Martin, & Conrad, 1959) using the height of the I_{200} (characterizes both crystalline and amorphous material, $2\theta = 22.7°$) and I_{am} (the minimum between the peaks at (2 0 0) and (1 1 0) represents only amorphous material ~18°) described:

$$\mathrm{CI} = \frac{I_{200} - I_{am}}{I_{200}} \times 100$$

The average thickness of the cellulose crystallites was calculated via Scherrer equation (Scherrer, 1918) measuring the full width at half-maximum (fwhm) of the θ_{max} (2 0 0) peak shown in:

$$D\ \ (\mathrm{nm}) = \frac{K\lambda}{\Delta 2\theta \cos\theta}$$

where D is the mean size of the crystallite in nanometer, $\Delta 2\theta$ is the full width as half maximum (fwhm) value, θ_{max} is maximum point in radians, K is Scherrer constant (0.94) and λ is X-ray wavelength.

Some new parameters were introduced to describe the degradation and decrystallization reactions by single quantitative parameters: Total weight of the amorphous cellulose (TAC) (g) was defined as the sum of the amorphous phase in the residue (measured by XRD) and the weight of the de-polymerized cellulose (weighted gravimetrically). It is assumed that only amorphous cellulose is de-polymerized.

$$\mathrm{TAC}\ \ (\mathrm{g}) = (\text{weight of amorphous phase in residue} + \text{weight of depolymerized cellulose})$$

Total amorphous area (TAA) was defined as the W/W percent of the total amorphous area to total weight of original cellulose:

$$\mathrm{TAA}\ \ (\%) = \left(\frac{\text{total weight of amorphcellulose}}{\text{total weight of cellulose}}\right) \times 100$$

Decrystallized area (DCA) is the weight of crystal area which turned to the amorphous structure during the microwave irradiation (the weight of original amorphous cellulose was measured by XRD):

$$\mathrm{DCA}\ \ (\mathrm{g}) = (\mathrm{TAC} - \text{weight of original amorphous cellulose})$$

Decrystallization efficiency (DCE) is the weight ratio of decrystallized area (DCA) to the total weight of original cellulose:

$$\mathrm{DCE} = \left(\frac{\text{Decrystallized area}}{\text{weight of original crystal cellulose}}\right) \times 100$$

3. Results and discussions

A highly effective process for liquefaction of cellulose by microwave-assisted reaction was developed by systematically investigating the effect of catalyst, time, temperature, sample amount and catalyst concentration. In addition, the effect of processing conditions on the degradation products was

fingerprinted to develop a process for selective production of glucose or levulinic acid. Our results demonstrate that exceptional liquefaction yields and high chemo-selectivity can be achieved under relatively mild temperature–chemical conditions by utilizing the synergistic effect of dilute acid catalyst and microwave irradiation to break the hydrogen bonding interactions in cellulose. The acid catalyzed microwave-assisted degradation process sketched based on the experimental results is schematically presented in Fig. 1. The process starts by the disruption of the hydrogen bonding and cellulose crystallinity, continues with depolymerization of cellulose to glucose and finally ends with further degradation of glucose to levulinic and formic acid (FA) through hydroxymethyl furfural (HMF) as the degradation intermediate. In addition carbonized structures are formed by polymerization of HMF.

3.1. Optimization of the liquefaction yield

As a first step to optimize the microwave-assisted reaction different catalysts (H_2SO_4, NaOH, LeA and PTSA) were evaluated and the reaction efficiency was compared to non-catalyzed reaction at the moderate reaction temperature of 140 °C. These results highlighted the efficiency of sulfuric acid in combination with microwave irradiation. Already during the initial trials liquefaction yields of ~50% were achieved during 120 min reaction with dilute sulfuric acid (0.01 g/ml) as a strong mineral acid catalyst in combination with microwave irradiation. The reaction with other catalysts resulted at maximum 34% liquefaction. Pure hydrothermal degradation without a catalyst was not observed under these conditions. The results are shown in more detail in the supporting information, Table S1.

To fully utilize the observed synergistic effect of acidic catalyzed microwave-assisted reaction, the process was further optimized with respect to temperature (T, °C), time (t, min), amount of cellulose (C, g) and acid concentration (A, g/ml). The highest liquefaction yield of 87%, based on the amount of solid residue, was achieved after 2 h at 160 °C. Increasing the temperature to 180 °C resulted in a slight reduction of liquefaction yield, which is explained by carbonization reaction through polymerization of HMF leading to formation of solid products. The effect of time was not unanimous, which is explained by concurring depolymerization, polymerization and carbonization reactions, forming new insoluble fractions (Xiao, Guo, Liang, & Qi, 2010; Yamada, Aratani, Kubo, & Ono, 2007). In general, however, longer degradation time resulted in higher liquefaction yield.

Evaluation of different sulfuric acid concentrations showed, interestingly, that the lowest sulfuric acid concentration of 0.0025 g/ml corresponding to 0.25 (w/w)% to water and 10% to cellulose, resulted in the highest liquefaction yield. Again polymerization and/or carbonization reactions together with the lower microwave power absorption ability (Kingston & Jassie, 1986), are likely explanation for the lower liquefaction yield at high sulfuric acid concentration. Increasing the sample concentration, on the other hand, generally resulted in higher liquefaction yield. The liquefaction yields and the effect of processing conditions are presented in Table S2 in supporting information and further discussed under the NMR quantification of the organic water-soluble degradation products (see Section 3.3).

3.2. LDI-MS fingerprinting of liquefaction products

The products formed through depolymerization and further degradation reactions under different conditions were fingerprinted by matrix-free LDI-MS, Fig. 2. The LDI-MS analysis showed a clear trend as a function of temperature where glucose, detected

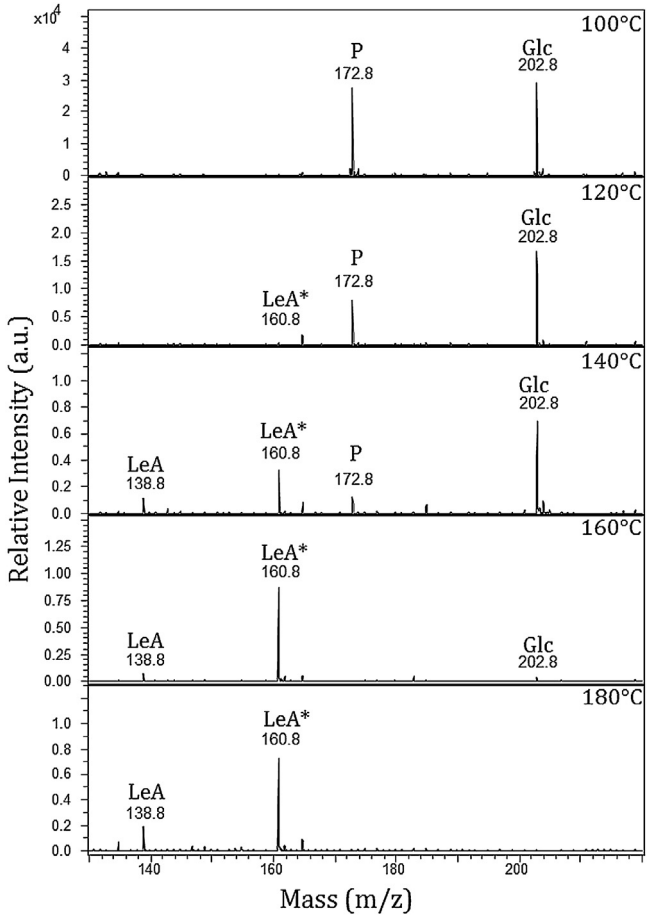

Fig. 2. LDI-MS spectra of liquefaction products after microwave heating at 100 °C, 120 °C, 140 °C, 160 °C and 180 °C. LeA = $[LeA+Na]^+$, LeA* = $[LeA-H+2Na]^+$, P = $[P+Na]^+$ and Glc = $[Glc+Na]^+$.

as a sodium adduct $[Glc+Na]^+$, was shown to be the main degradation product at lower temperatures (100 and 120 °C). The highest signal-to-noise ratio for glucose was observed at 120 °C, which indicates the highest glucose yield after reaction at 120 °C. 140 °C was the turning point where glucose and levulinic acid co-existed. At higher temperatures (160 and 180 °C) glucose rapidly degraded and two intensive peaks, $[LeA+Na]^+$ and $[LeA-H+2Na]^+$, both corresponding to levulinic acid were observed. The degradation products were further verified by ESI-MS analysis, which confirmed the products identified by LDI-MS (results not shown). Similar trends were observed when the effect of reaction time, sample amount and acid concentration were evaluated. Glucose formation dominated under mild reaction conditions and when the reaction time was short, whereas prolonged reaction or harsher conditions led to the formation of high amounts of levulinic acid. The used cellulose originally contained small amounts of Xylan (pentose). Xylan is expected to be present in the amorphous regions of the material and is, thus, easily hydrolyzed to pentose and rapidly extracted into the liquefaction solvent. Accordingly pentose was detected in the LDI-MS spectra (marked P). It had high relative intensity when the liquefaction yield was low, but its relative intensity in relation to the other products decreased as the liquefaction yield increased.

The semi-quantitative LDI-MS results, thus, indicate the presence of intervals inside which depolymerization and/or further degradations reactions dominate leading to glucose or levulinic acid as the main final liquefaction products, respectively. In addition formic acid is formed as a co-product from levulinic acid formation (see Section 3.3).

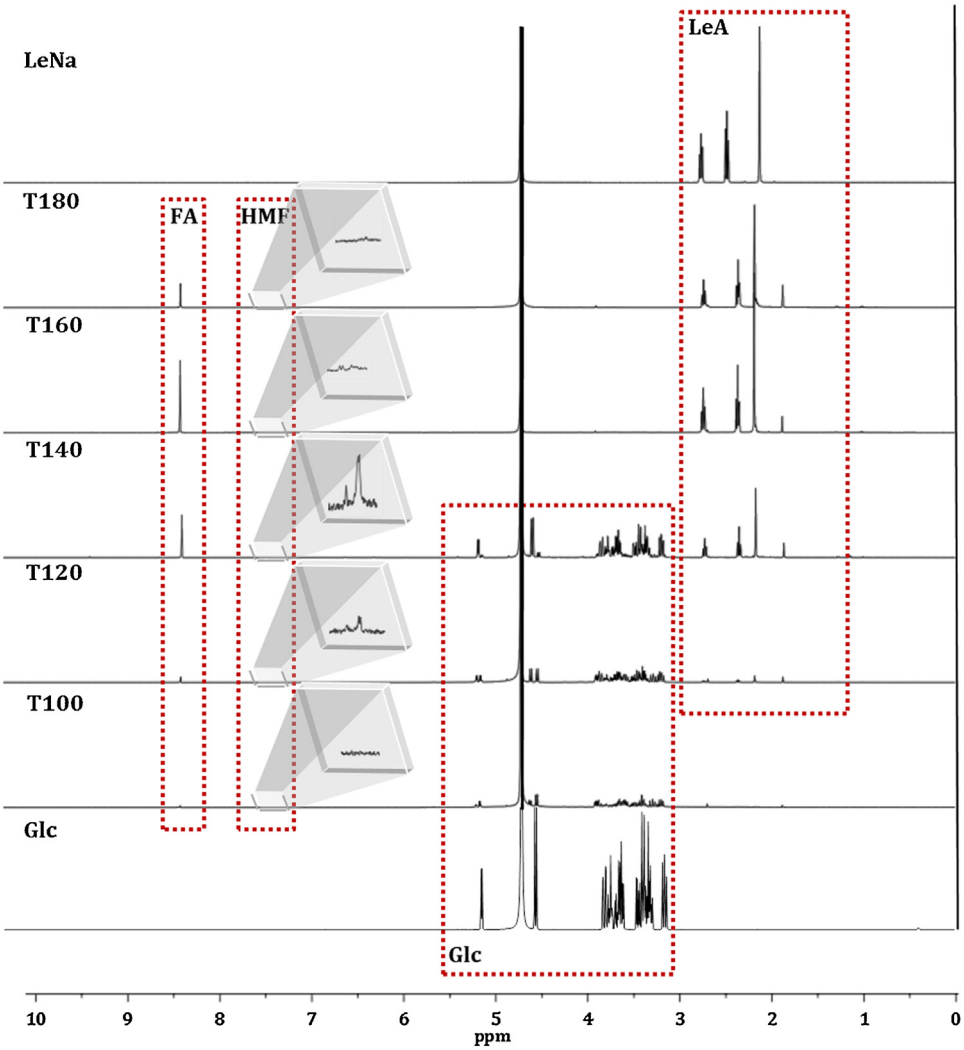

Fig. 3. ^{1}H NMR spectra of the liquefaction products after microwave irradiation at different temperatures (100, 120, 140, 160 and 180 °C) and reference spectra for pure levulinic acid (LeA) and glucose (Glc).

3.3. Quantitative determination of liquefaction products by NMR

^{1}H and ^{13}C NMR spectra confirmed the LDI-MS identification of the liquefaction products (Fig. 3 and Figs. S1–S8). Fig. 3 shows as an example the NMR spectra of the products formed after 120 min reaction at different temperatures varying from 100 °C to 180 °C. In accordance with LDI-MS results, depending on the reaction temperature, glucose or levulinic acid was identified as the main degradation product. Both sodium levulinate (LeNa) and levulinic acid were observed in the NMR spectra (see Fig. 3 and Figs. S4–S8 of SI file) due to the neutralization step and equilibrium of weak acids (Fig. S3). Small amount of HMF, an intermediate of glucose degradation, was also observed in some cases. The amount was, however, always low indicating rapid further degradation to levulinic acid and/or participation in carbonization reactions. Theoretically formic acid, a co-product from levulinic acid formation, is formed in 1:1 molar ratio to levulinic acid. However, the amount of formic acid detected in the NMR spectra was in most cases somewhat smaller and not totally reproducible, which was probably due to losses during the processing of the liquefaction products. It can also be noted that a mixture of glucose isomers (α and β) were detected in the NMR spectra (Fig. S3, Table S1). The high selectivity of the reaction, leading in most cases to either glucose or levulinic acid formation, was clearly shown both by the LDI-MS and NMR analysis. The only exception was the reaction at 140 °C, where a turning point from glucose to levulinic acid production was observed resulting in a mixture of degradation products.

The effect of reaction parameters, temperature, time, cellulose amount and catalyst concentration, on the liquefaction yield and amount of degradation products is further demonstrated in Fig. 4. This figure gives the relative molar yield of glucose, HFM and levulinic acid as a percentage of the theoretical maximum yield. The theoretical relative molar yield of formic acid corresponds to relative molar yield of levulinic acid as each repeating unit in original cellulose degrades to one levulinic acid and one formic acid molecule. Due to the closeness of the molar mass of cellulose repeating unit and the resulting degradation products, these molar fraction correspond closely to the weight fraction of the different products (if the molar fraction of levulinic acid is replaced by weight fraction of levulinic acid and formic acid). The red triangles illustrate the liquefaction yield derived from the amount of remaining solid material. The rather abrupt turning point, when approximately 50% liquefaction was achieved, is clearly observed. Under mild reaction conditions and liquefaction yields up to ~50%, depolymerization was the dominating reaction and glucose was formed almost as the sole degradation product with high selectivity and purity. Typically 40–50% of the original cellulose units could be depolymerized to glucose.

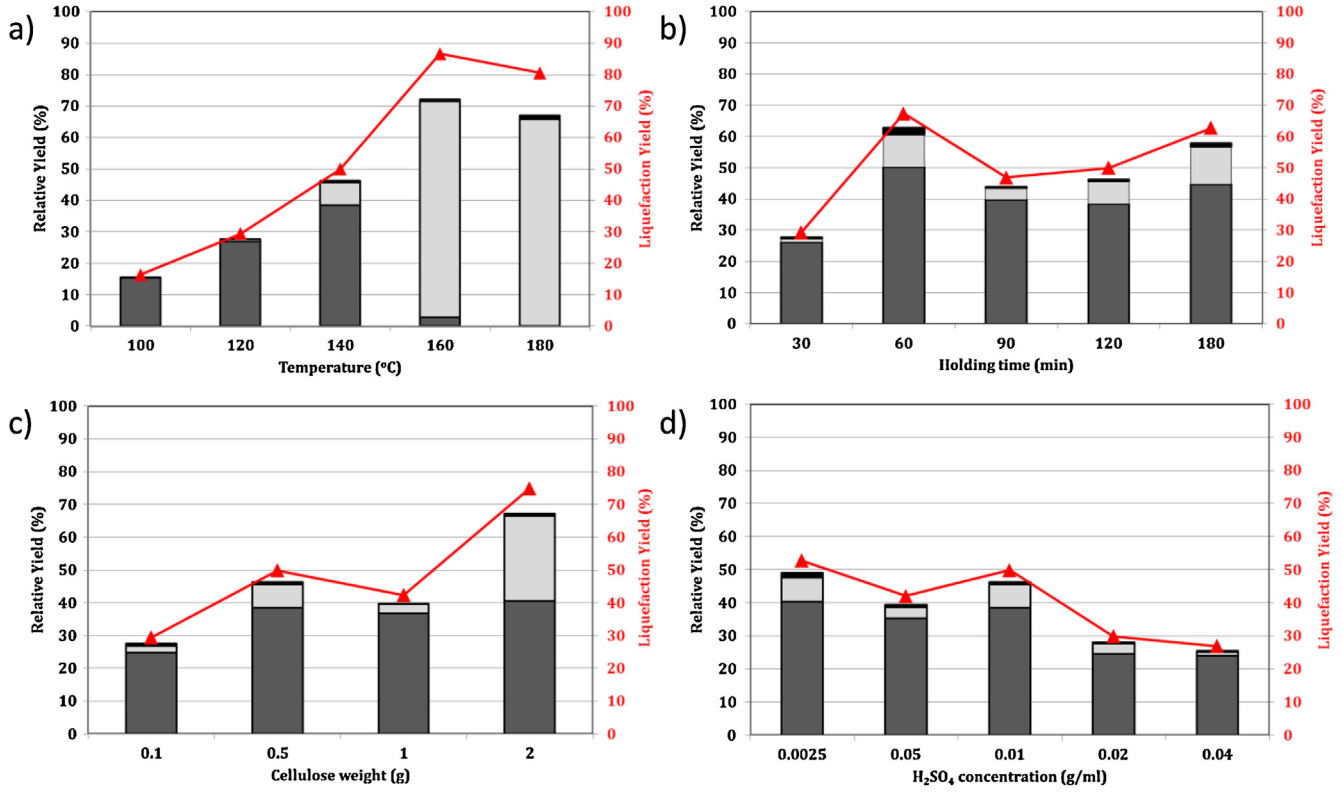

Fig. 4. The liquefaction yields and composition of water-soluble liquefaction products detected by NMR (a) at different temperatures, (b) after different holding times, (c) with different amount of cellulose and (d) with different H_2SO_4 concentrations. Liquefaction yield (red triangle), relative yield (%) of Glc (dark grey), LeA (light grey) and HMF (black). (For interpretation of the references to color in this figure legend, the reader is referred to the web version of this article.)

At high liquefaction yield, glucose was rapidly and with high selectivity further degraded via HMF to levulinic acid and its co-product formic acid. This phenomenon was generally observed when the liquefaction yield was above 45–50%, irrespective whether this was achieved by increasing temperature, time or by changing some of the other processing parameters. At the temperature curve this turning point was observed at 140 °C. The high yield was connected to the formation of solid carbonized structures due to polymerization of HMF.

Fig. 4a further demonstrates that the highest liquefaction yield of 87%, as determined from the amount of solid residue, was obtained at 160 °C. At this temperature the relative molar yield of levulinic acid was 69%, meaning that 69% of the original cellulose repeating units were converted to levulinic acid and formic acid. The amount of levulinic acid after 120 min of liquefaction at 160 °C was almost identical to the amount obtained after 120 min at 180 °C. However, the small amount of glucose present after degradation at 160 °C had reacted further, which together with the almost constant levulinic acid concentration indicates polymerization or carbonization–precipitation processes. The most efficient glucose production temperature was 140 °C, while the most selective glucose production (99% selectivity) was achieved at 100 °C. The time dependence of the reaction proceeding at 140 °C shown in Fig. 4b illustrates that purest glucose was obtained by utilizing a short heating time of 30 min. The highest liquefaction yield, on the other hand, was achieved after 60 min. The influence of original cellulose concentration shown in Fig. 4c indicates that higher amount of cellulose leads to higher liquefaction yield and higher amount of levulinic acid. The increased ratio of cellulose to the sulfuric acid reduced the dehydration and polymerization of HMF and favored the further degradation to LeA and FA. Observations concerning the catalyst concentration in Fig. 4d demonstrate that increasing sulfuric acid concentration leads to lower liquefaction efficiencies and higher selectivity towards glucose. Higher sulfuric acid concentration probably enhances the dehydration and polymerization of HMF resulting in formation of solid carbon spheres. Altogether the obtained liquefaction yields and the chemo-selective production of glucose and/or levulinic acid are exceptionally high as compared to previous results from literature.

At lower liquefaction yields the total weight of organic liquefaction products correlated closely to the liquefaction yield obtained from the amount of solid residue. After reaction at 160 °C and 180 °C, no residues of the original cellulose were observed. Instead the solid residue consisted of amorphous carbon spheres formed through polymerization of HMF (see Sections 3.4 and 3.5). This carbonization reaction includes dehydration reactions leading to release of small compounds, mostly water, not detectable in the NMR spectra. This fraction is expected to be responsible for the difference observed between the yield of organic liquefaction products and the liquefaction yield calculated from the solid residue (Fig. 4). Accordingly this difference was mainly observed when the liquefaction yield was high and carbonization reactions had taken place.

Fig. 5 shows the contour curves drawn to further illustrate the reaction conditions for the highest liquefaction yield as well as the conditions for highest glucose or levulinic acid production. For example degradation for 60 min at 140 °C using 0.5 g cellulose and 0.05 g H_2SO_4, led to reasonable liquefaction efficiency and high amount of glucose in a short reaction time. The ratios of the produced materials emphasize the optimized condition for pure depolymerization of glucose at the lower time-temperature region. Harsher conditions favor the further

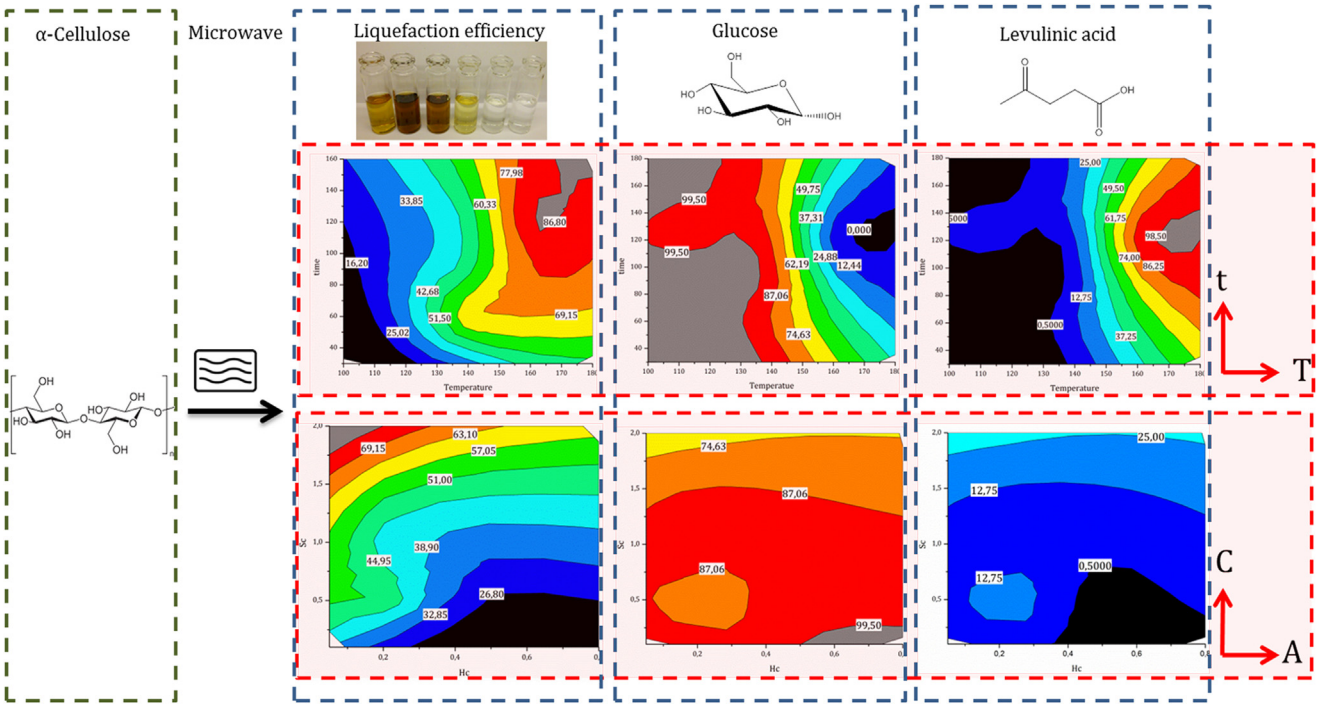

Fig. 5. Contour curves demonstrating the conditions for maximum liquefaction yield and maximum glucose or levulinic and formic acid formation.

degradation of glucose to levulinic acid and its co-product formic acid.

3.4. Characterization of the liquefaction residue

The liquefaction time and temperature had a pronounced effect on the physical appearance of the remaining residue. Fig. 6 illustrates the size and morphology of the original cellulose fibers and the liquefaction residues after 120 min. liquefaction at different temperatures. After liquefaction at 100 °C the original cellulose fibers were still well preserved. However, some erosion of amorphous material from the surface of the fibers could be detected. 140 °C was again shown to be a turning point, where significant degradation of cellulose fibers starts. At 180 °C the cellulose fiber structure was totally lost and the remaining residue had a shape of small spherical micro-and nano-sized particles indicating carbonization.

3.5. Crystallinity of the liquefaction residue

XRD was utilized to follow the crystallinity and crystal thickness in the remaining solid cellulose residues and to depict the interaction of cellulose with the acidic solution during microwave irradiation (Fig. 7). The diffraction pattern of native cellulose I is obvious in the X-ray diffractogram shown in Fig. 7 (top), $2\theta = 14.8–16.3^{o}$ (reflection assigned to the $(1\,\bar{1}\,0)$ and $(1\,1\,0)$ crystallographic plane), the $2\theta = 18.30–18.40^{o}$ (reflection assigned to the amorphous phase) and $2\theta = 21.90–22.20^{o}$ (reflection assigned to the $(2\,0\,0)$ crystallographic plane) (Poletto, Zattera, Forte, & Santana, 2012) (Fig. 7).

Using Segal and Scherrer methods, the original α-cellulose I had a crystallinity index (CI) of 64.2% and amorphous index of 35.8%. The crystal thickness was 3.1 nm (Fig. 8). During liquefaction at 100 °C some crystal thickening took place at the same time as the crystallinity index of the samples slightly increased probably due to the liquefaction of the amorphous regions, which allowed some recrystallization in the amorphous regions (Bhuiyan, Hirai, & Sobue, 2000; Bhuiyan & Hirai, 2005) (Fig. 8). The degradation of amorphous parts is also seen as surface erosion in the SEM images (Fig. 6b). The liquefaction at 100 °C was limited to the amorphous parts of the material. However, during liquefaction at higher temperatures, the process was able to break the strong secondary bonding and the decrystallization of the cellulose fibers was initiated. This led to significantly higher liquefaction yields already at 140 °C and temperatures above this. The exceptionally high liquefaction efficiency and yield at 160 and 180 °C led to formation of spherical carbonized residues (Chundawat et al., 2011) and was accompanied with dramatic changes in morphology and XRD pattern (Figs. 6d and 7e and f). In addition to the easily hydrolysable amorphous regions in the cellulose, the synergistic combination of acidic conditions and microwave irradiation was able to break hydrogen bonding in the crystalline regions. This in turn reduced the crystallinity and provided more space for water to attack 1–4 glycosidic bonds, as a consequence the hydrolysis reaction could proceed (Fan et al., 2013).

3.6. Visible examination and UV analysis

The visible examination of the liquefied product mixtures and solid residues showed a yellow-brownish color, which gradually became more intense as the degradation continued. This is illustrated in the picture included in Fig. 5 and Fig. S9 in the supporting information. In correlation with the visual observations, the presence of levulinic acid and HMF was also shown by UV–vis survey. Glucose does not have significant absorption at the UV–vis region. The characteristic absorption of HMF and levulinic acid is at wavelength of 284 nm and 266 nm (λ_{max} (H_2O)), respectively. The absorption of HMF and levulinic acid followed Beer's law very well (supporting information, Fig. S10) and it correlated linearly to levulinic acid and HMF concentration. As expected the molar absorptivity of HMF was higher in comparison to molar absorptivity of levulinic acid.

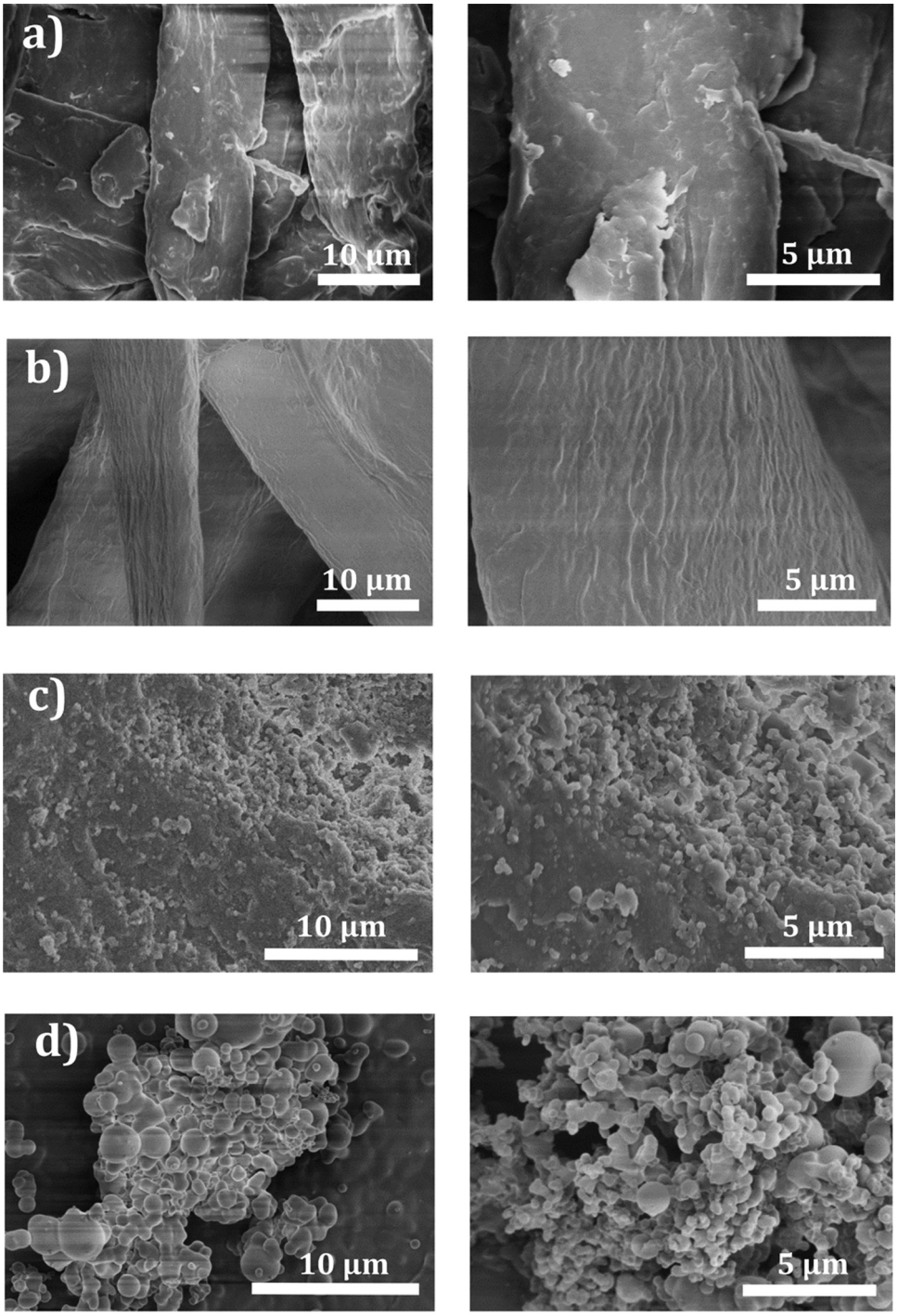

Fig. 6. SEM images showing the size and shape of (a) the original cellulose fibers and the liquefaction residues after 120 min at (b) 100 °C (c) 140 °C and (d) 180 °C.

3.7. FTIR analysis of the liquefaction residues

FTIR spectra of the liquefaction residues showed changes in the functional groups as compared to the FTIR spectra of the original cellulose (Figs. S11 and S12). The boosted liquefaction and glucose degradation at the temperatures higher than 120 °C resulted in the formation of new functional groups, such as carbonyl and aromatic groups (1-alcohol O—H stretching or/and carboxylic acid O—H stretching, 2-aromatic C=C bending and C=O stretching at 1500–1750 cm^{-1} and 3-peaks in the region 1000–1260 cm^{-1} C—O stretching), which indicates that degradation-carbonization reactions have taken place in the solid residues (Fig. S11). The FTIR and XRD analysis showed the preservation of the cellulose I pattern up to liquefaction temperature of 140 °C. However, the pattern totally disappeared after liquefaction at 160 °C and 180 °C, which further indicates carbonization. FTIR spectra of the

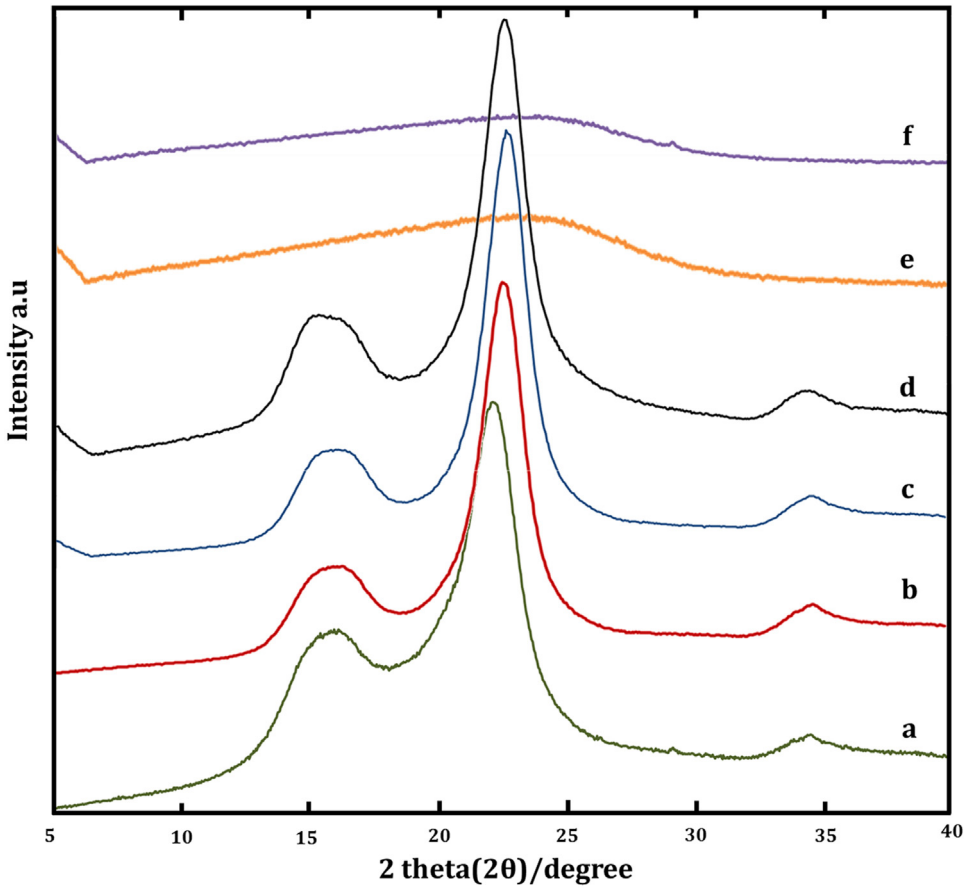

Fig. 7. X-ray diffraction pattern of (a) pure α-cellulose at 25 °C and the liquefaction residues after 120 min at (b) 100 °C, (c) 120 °C, (d) 140 °C, (e) 160 °C and (f) 180 °C.

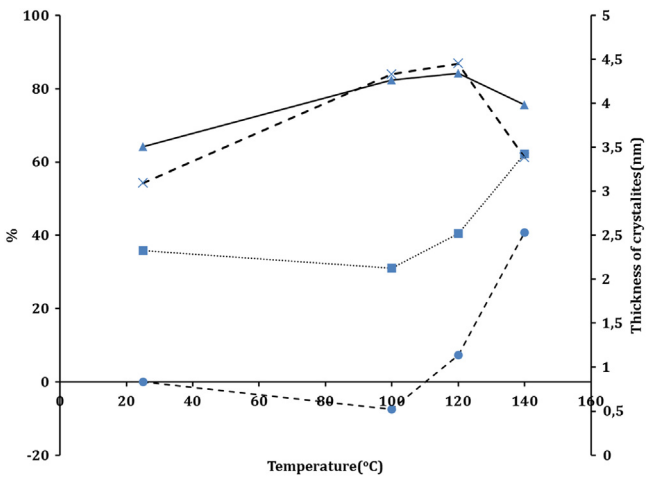

Fig. 8. Decrystallization behavior of the cellulose at different temperatures under microwave degradation (25 °C is pure α-cellulose) total amorphous area (■), crystallized area at the solid materials (▲), Decrystallization efficiency (●) and thickness of the crystallites (×).

liquefied materials exhibited functional group absorption corresponds to glucose, levulinic and formic acids depending on the liquefaction temperature.

4. Conclusions

Exceptionally effective and chemo-tunable process for liquefaction of cellulose was developed by utilizing the synergistic effect of acid catalyzed reaction and microwave-assisted process, which could disrupt the strong secondary bonds in cellulose. Liquefaction yields as high as 87%, as determined from the remaining solid residue, were reached and the liquefaction products could be controlled with 98–99% selectivity towards glucose or levulinic and formic acid production. Relative molar yields up to 50 and 69% were reached for glucose and levulinic acid, respectively. Almost pure depolymerization to glucose was achieved under mild liquefaction condition with up to 45–55% liquefaction yields. At higher liquefaction yields glucose was rapidly and almost quantitatively further degraded to levulinic acid. This further degradation was accompanied with carbonization leading to formation of small spherical residues, carbon spheres.

Notes

Electronic Supplementary Information (ESI) available: qualitative and quantitative analysis of the liquefied products and residues, ^{1}H and ^{13}C NMR spectra, UV–vis, images of liquefied samples and typical FT-IR spectra.

Acknowledgements

The Swedish Research Council (VR) is acknowledged for financial support (contract grant number 2012-4369).

Appendix A. Supplementary data

Supplementary data associated with this article can be found, in the online version, at http://dx.doi.org/10.1016/j.carbpol.2014.06.011.

References

Allan, G. G., Krieger, B. B., & Work, D. W. (1980). Dielectric loss microwave degradation of polymers: Cellulose. *Journal of Applied Polymer Science*, *25*(9), 1839–1859.

Azwar, E., Yin, B., & Hakkarainen, M. (2013). Liquefied biomass derived plasticizer for polylactide. *Journal of Chemical Technology & Biotechnology*, *88*(5), 897–903.

Bhuiyan, M. T., Hirai, N., & Sobue, N. (2000). Changes of crystallinity in wood cellulose by heat treatment under dried and moist conditions. *Journal of Wood Science*, *46*(6), 431–436.

Bhuiyan, T. R., & Hirai, N. (2005). Study of crystalline behavior of heat-treated wood cellulose during treatments in water. *Journal of Wood Science*, *51*(1), 42–47.

Bobleter, O., Niesner, R., & Röhr, M. (1976). The hydrothermal degradation of cellulosic matter to sugars and their fermentative conversion to protein. *Journal of Applied Polymer Science*, *20*(8), 2083–2093.

Carrasco, J. E., Sáiz, M., Navarro, A., Soriano, P., Sáez, F., & Martinez, J. M. (1994). Effects of dilute acid and steam explosion pretreatments on the cellulose structure and kinetics of cellulosic fraction hydrolysis by dilute acids in lignocellulosic materials. *Applied Biochemistry and Biotechnology*, *45–46*(1), 23–34.

Chheda, J. N., Huber, G. W., & Dumesic, J. A. (2007). Liquid-phase catalytic processing of biomass-derived oxygenated hydrocarbons to fuels and chemicals. *Angewandte Chemie International Edition*, *46*(38), 7164–7183.

Chundawat, S. P. S., Bellesia, G., Uppugundla, N., da Costa Sousa, L., Gao, D., Cheh, A. M., et al. (2011). Restructuring the crystalline cellulose hydrogen bond network enhances its depolymerization rate. *Journal of the American Chemical Society*, *133*(29), 11163–11174.

Fan, J., De bruyn, M., Budarin, V. L., Gronnow, M. J., Shuttleworth, P. S., Breeden, S., et al. (2013). Direct microwave-assisted hydrothermal depolymerization of cellulose. *Journal of the American Chemical Society*, *135*(32), 11728–11731.

Hendriks, A. T. W. M., & Zeeman, G. (2009). Pretreatments to enhance the digestibility of lignocellulosic biomass. *Bioresource Technology*, *100*(1), 10–18.

Himmel, M. E., Ding, S.-Y., Johnson, D. K., Adney, W. S., Nimlos, M. R., Brady, J. W., et al. (2007). Biomass recalcitrance: Engineering plants and enzymes for biofuels production. *Science*, *315*(5813), 804–807.

Hilgert, J., Meine, N., Rinaldi, R., & Schuth, F. (2013). Mechanocatalytic depolymerization of cellulose combined with hydrogenolysis as a highly efficient pathway to sugar alcohols. *Energy & Environmental Science*, *6*(1), 92–96.

Huang, Y.-B., & Fu, Y. (2013). Hydrolysis of cellulose to glucose by solid acid catalysts. *Green Chemistry*, *15*(5), 1095–1111.

Kingston, H. M., & Jassie, L. B. (1986). Microwave energy for acid decomposition at elevated temperatures and pressures using biological and botanical samples. *Analytical Chemistry*, *58*(12), 2534–2541.

Knill, C. J., & Kennedy, J. F. (2003). Degradation of cellulose under alkaline conditions. *Carbohydrate Polymers*, *51*(3), 281–300.

Kržan, A., & Žagar, E. (2009). Microwave driven wood liquefaction with glycols. *Bioresource Technology*, *100*(12), 3143–3146.

Lin, L. Z., Yao, Y. G., Yoshioka, M., & Shiraishi, N. (2004). Liquefaction mechanism of cellulose in the presence of phenol under acidic catalysis. *Carbohydrate Polymers*, *57*(2), 123–129.

Liu, F., Kamat, R. K., Noshadi, I., Peck, D., Parnas, R. S., Zheng, A., et al. (2013). Depolymerization of crystalline cellulose catalyzed by acidic ionic liquids grafted onto sponge-like nanoporous polymers. *Chemical Communications*, *49*(76), 8456–8458.

Matson, T. D., Barta, K., Iretskii, A. V., & Ford, P. C. (2011). One-pot catalytic conversion of cellulose and of woody biomass solids to liquid fuels. *Journal of the American Chemical Society*, *133*(35), 14090–14097.

Moller, M., Harnisch, F., & Schroder, U. (2013). Hydrothermal liquefaction of cellulose in subcritical water – the role of crystallinity on the cellulose reactivity. *RSC Advances*, *3*(27), 11035–11044.

Monier-Williams, G. W. (1921). XC.-The hydrolysis of cotton cellulose. *Journal of the Chemical Society Transactions*, *119*(0), 803–805.

Ogihara, Y., Smith, R., Jr., Inomata, H., & Arai, K. (2005). Direct observation of cellulose dissolution in subcritical and supercritical water over a wide range of water densities (550–1000 kg/m^3). *Cellulose*, *12*(6), 595–606.

Pinkert, A., Marsh, K. N., Pang, S., & Staiger, M. P. (2009). Ionic liquids and their interaction with cellulose. *Chemical Reviews*, *109*(12), 6712–6728.

Poletto, M., Zattera, A. J., Forte, M. M. C., & Santana, R. M. C. (2012). Thermal decomposition of wood: Influence of wood components and cellulose crystallite size. *Bioresource Technology*, *109*(0), 148–153.

Ritter, G. J., Mitchell, R. L., & Seborg, R. M. (1933). Some factors that influence the conversion of cellulosic materials to sugars. *Journal of the American Chemical Society*, *55*(7), 2989–2991.

Sasaki, M., Fang, Z., Fukushima, Y., Adschiri, T., & Arai, K. (2000). Dissolution and hydrolysis of cellulose in subcritical and supercritical water. *Industrial & Engineering Chemistry Research*, *39*(8), 2883–2890.

Scherrer, P. (1918). Bestimmung der Größe und der inneren Struktur von Kolloidteilchen mittels Röntgenstrahlen. Nachrichten von der Gesellschaft der Wissenschaften zu Göttingen. *Mathematisch-Physikalische Klasse*, *1918*, 98–100.

Segal, L., Creely, J. J., Martin, A. E., & Conrad, C. M. (1959). An empirical method for estimating the degree of crystallinity of native cellulose using the X-ray diffractometer. *Textile Research Journal*, *29*(10), 786–794.

Sequeiros, A., Serrano, L., Briones, R., & Labidi, J. (2013). Lignin liquefaction under microwave heating. *Journal of Applied Polymer Science*, *130*(5), 3292–3298.

Simonsen, E. (1898). Spiritus aus cellulose und Holz. *Angewandte Chemie*, *11*(9), 195–196.

Sun, Y., & Cheng, J. (2002). Hydrolysis of lignocellulosic materials for ethanol production: A review. *Bioresource Technology*, *83*(1), 1–11.

Szabolcs, A., Molnar, M., Dibo, G., & Mika, L. T. (2013). Microwave-assisted conversion of carbohydrates to levulinic acid: An essential step in biomass conversion. *Green Chemistry*, *15*(2), 439–445.

Takahashi, Y., & Matsunaga, H. (1991). Crystal structure of native cellulose. *Macromolecules*, *24*(13), 3968–3969.

Xiang, Q., Lee, Y. Y., Pettersson, P., & Torget, R. (2003). Heterogeneous aspects of acid hydrolysis of α-cellulose. *Applied Biochemistry and Biotechnology*, *107*(1–3), 505–514.

Xiao, H., Guo, Y., Liang, X., & Qi, C. (2010). One-step synthesis of novel biacidic carbon via hydrothermal carbonization. *Journal of Solid State Chemistry*, *183*(7), 1721–1725.

Yamada, T., Aratani, M., Kubo, S., & Ono, H. (2007). Chemical analysis of the product in acid-catalyzed solvolysis of cellulose using polyethylene glycol and ethylene carbonate. *Journal of Wood Science*, *53*(6), 487–493.